Supporting Information

Multi-functional groups decorated composite nanofiber separator with excellent chemical stability in ester-based electrolyte for enhancing the lithium-ion transport

Xin Xie[a,1], *Lei Sheng*[a,b,1], *Catia Arbizzani*[b], *Bin Gao*[a], *Xingxu Gao*[a], *Ling Yang*[a], *Yaozong Bai*[c], *Haoyu Dong*[c], *Gaojun Liu*[c], *Tao Wang*[a], *Xianli Huang*[a], *Jianping He*[a]*

[1] These authors contributed equally to this work.

[a] College of Material Science and Technology, Nanjing University of Aeronautics and Astronautics, 210016, Nanjing, Jiangsu Province, China.

[b] Department of Chemistry "Giacomo Ciamician", University of Bologna, 40126, Bologna, Italy

[c] Sinoma Lithium Battery Separator Co. Ltd, 277500, ZaoZhuang, Shandong province, China

*Corresponding author: *Jianping He*

Email address: jianph@nuaa.edu.cn;

Table of Contents

Figure S10 The top-view SEM images of (a-c) pristine PAN/CA composite nanofiber separators, (g-i) pristine PE separators. And the SEM images of (d-f) PAN/CA composited nanofiber separators and (j-l) PE separators disassembled from Li/Li symmetric cells after long-term cycles of Li plating/stripping process.

Figure S11 The top-view SEM images of fresh Li metal anodes (a-c), and the Li metal anodes obtained in $LiFePO_4$/Li half cells assembled with PAN/CA nanofiber separators (d-f) and PE separators (g-i) after cycle performance test.

Figure S12 The top-view SEM images of pristine $LiFePO_4$ electrodes (a-d); and the top-view SEM images of the $LiFePO_4$ electrodes obtained in $LiFePO_4$/Li half cells assembled with PAN/CA composite nanofiber separators (e-h) and PE separators (i-l) after cycle performance test.

Figure S13 CV curves of $LiCoO_2$/Li battery based on (a) PAN/CA composite nanofiber separator, (b) PAN nanofiber separator and (c) PE separator.

Figure S14 Capacity -Voltage curves with different separators under different cycles: (a) 1_{st} cycle; (b) 50_{th} cycle; (c) 150_{th} cycle.

Figure S15 Discharge capacity-voltage curves of $LiCoO_2$/Li cells assembled with PAN nanofiber separator.

Figure S16 Rate performance of $LiFePO_4$/Li cells assembled with PAN/CA composite nanofiber separator, PAN nanofiber separator and PE separator.

Figure S17 Charge-discharge voltage-time profiles of Li-symmetrical cells assembled with PAN/CA nanofiber separator and PE separator at current density of (a) 2 mA cm^{-2} with an areal capacity of 2 mAh cm^{-2}.

Table S1 Performance comparison between the separators in this work and those reported in the literature.

Table S2 Physical properties of PAN/CA nanofiber separator, PAN nanofiber separator and PE separator.

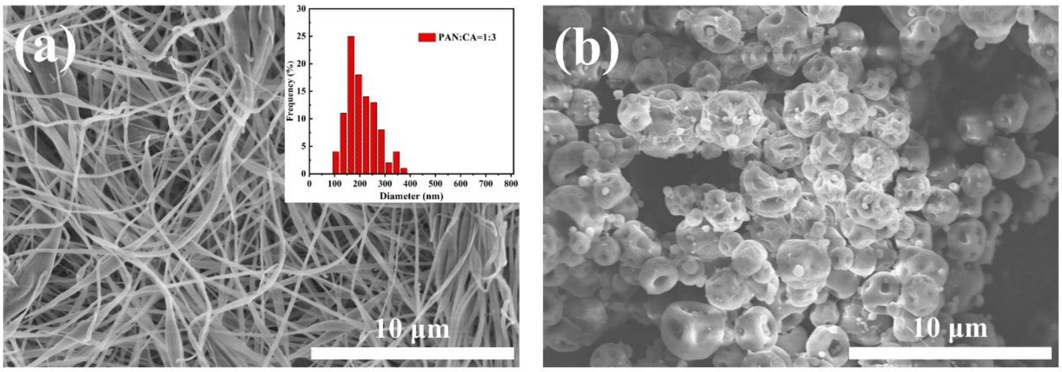

Figure S1. The top-view SEM images and diameter distributions of (a) PAN:CA=1:3, (b) pure CA.

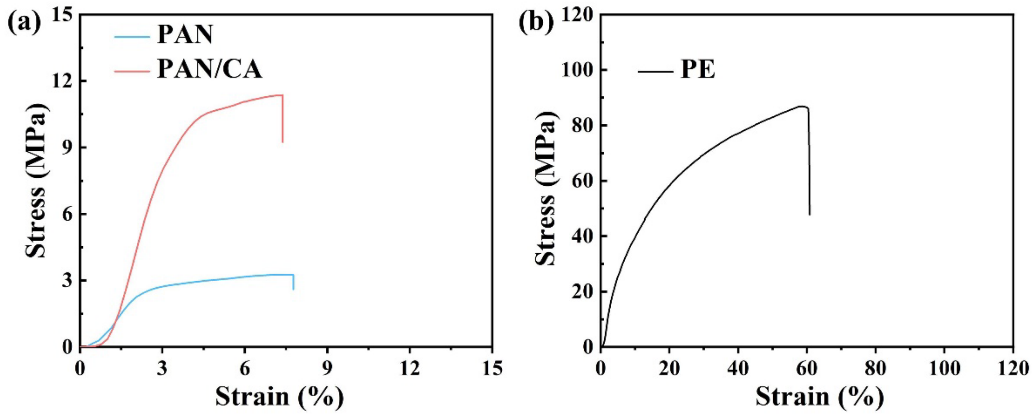

Figure S2. The stress-strain curves of PAN/CA nanofiber composite separator (a), PAN nanofiber separator (a) and PE separator (b).

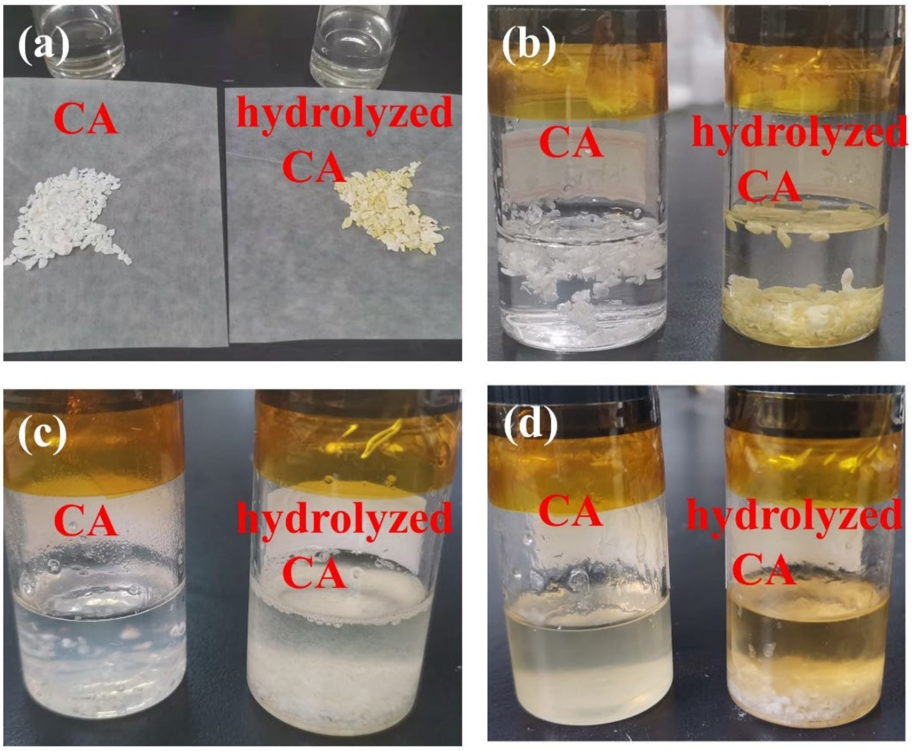

Figure S3. Stability test of CA and alkaline hydrolyzed CA in the liquid electrolyte: (a) pristine; (b) an hour; (c) 12 hours; (d) 24 hours.

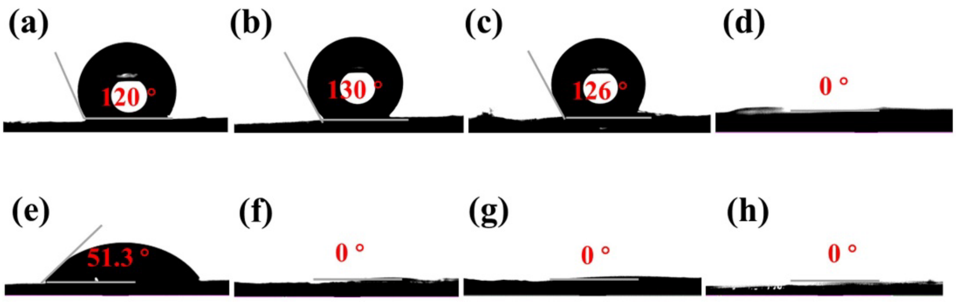

Figure S4. Contact angles with distilled water (a-d) and liquid electrolyte (e-h): (a) (e) PE, (b) (f) PAN, (c) (g) PAN/CA before hydrolysis treatment, (d) (h) PAN/CA after hydrolysis treatment.

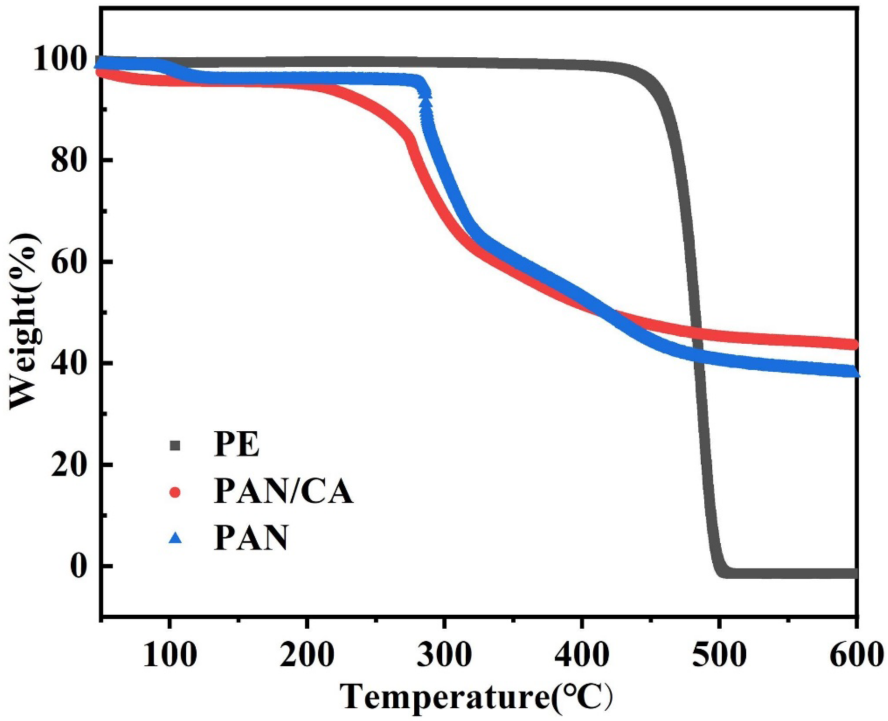

Figure S5. TGA curves of PE separator, PAN nanofiber separator and PAN/CA composite nanofiber separator.

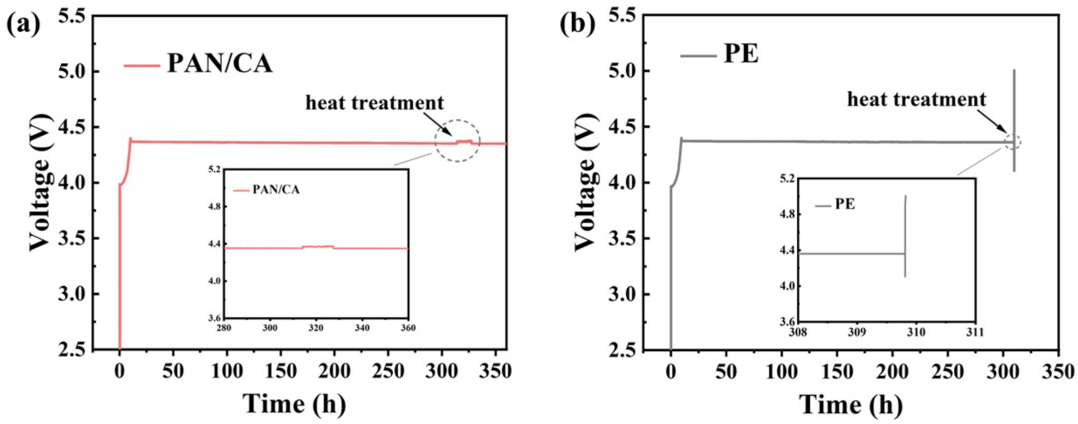

Figure S6. The voltage profiles of heat treatment test in a $LiCoO_2$/Li cell with (a) PAN/CA composite nanofiber separator and (b) PE separator. The heat treatment process was that the cells were placed in a preheated 55 ℃ vacuum drying box for 0.5 h.

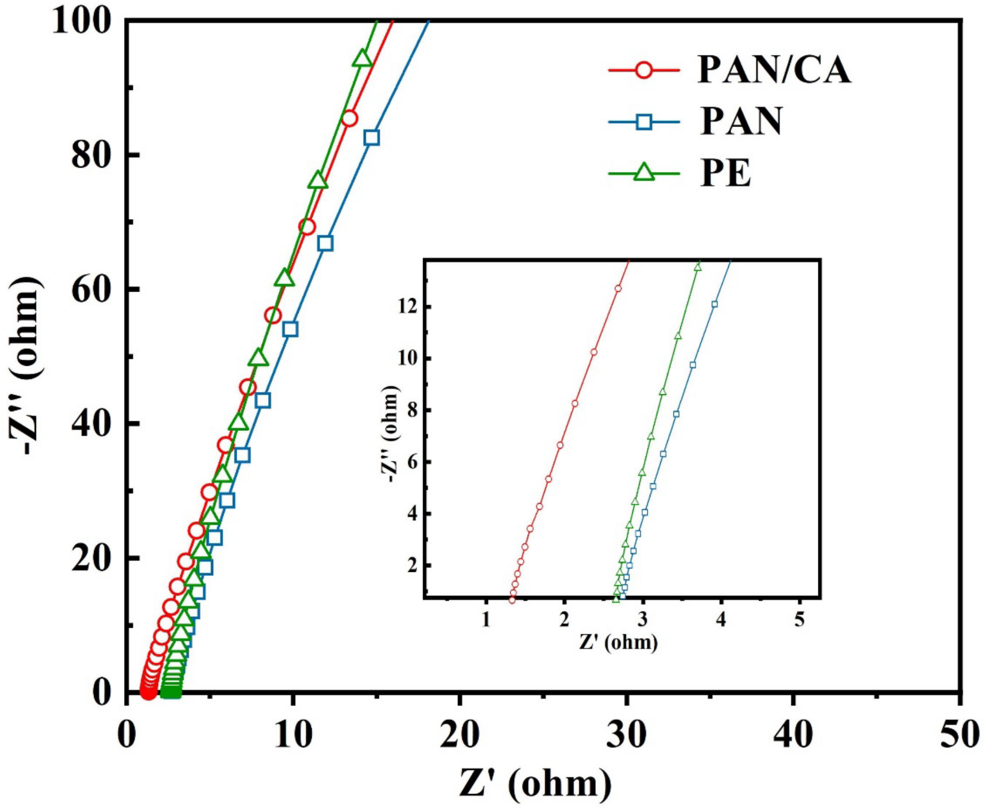

Figure S7. Nyquist plots of PAN/CA, PAN and PE separators assembled in SS symmetrical cells.

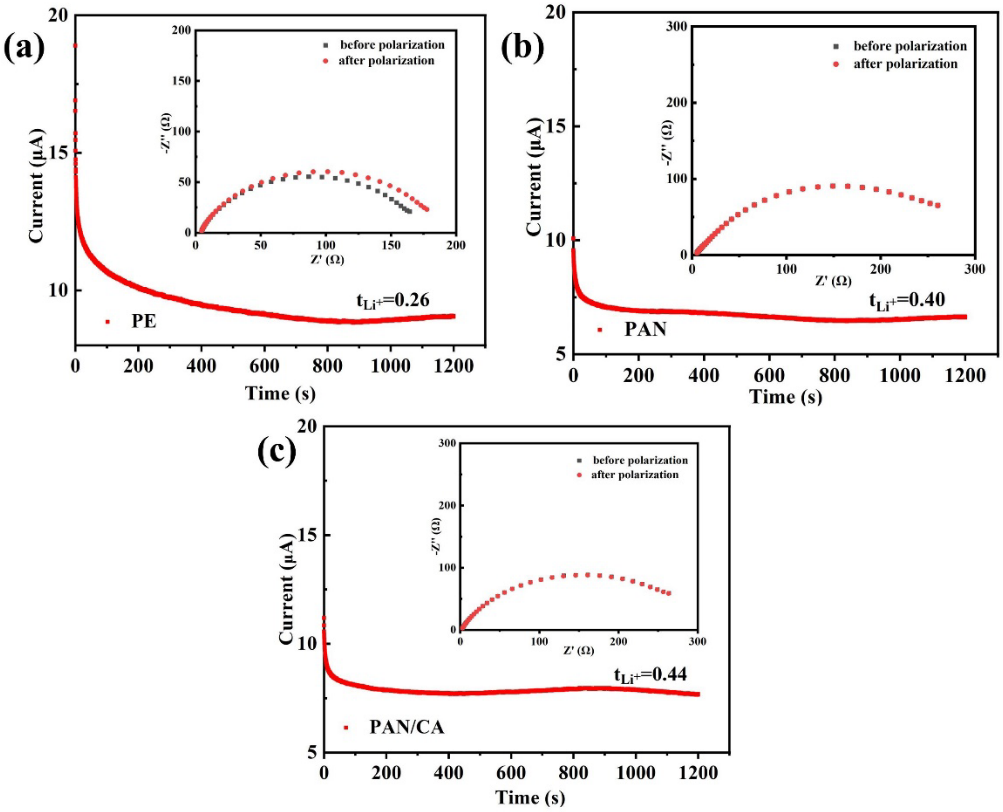

Figure S8. Steady-state current curves of (a) PE, (b) PAN, and (c) PAN/CA separator, and the Nyquist plots of the cells containing the corresponding separators before and after polarization.

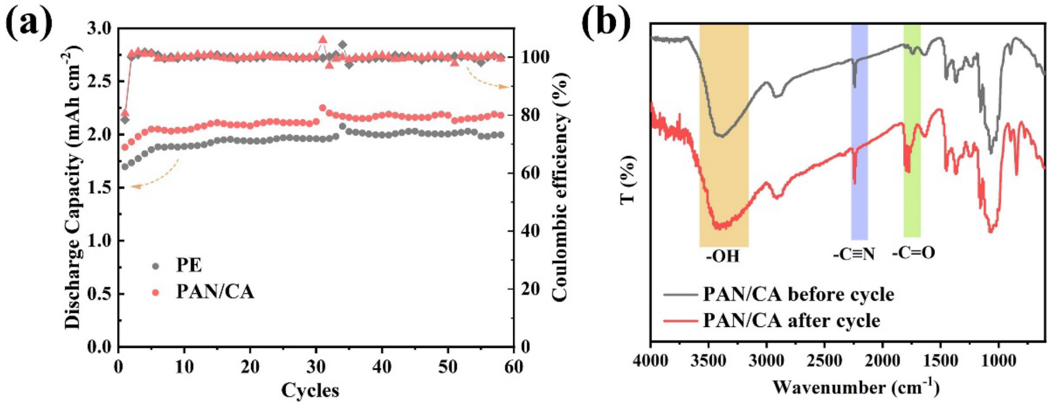

Figure S9. (a) Cycle performance of $LiFePO_4$/Li cells based on PAN/CA and PE separators at a current density of 1C; (b) FTIR spectra of PAN/CA separators before and after cycle test.

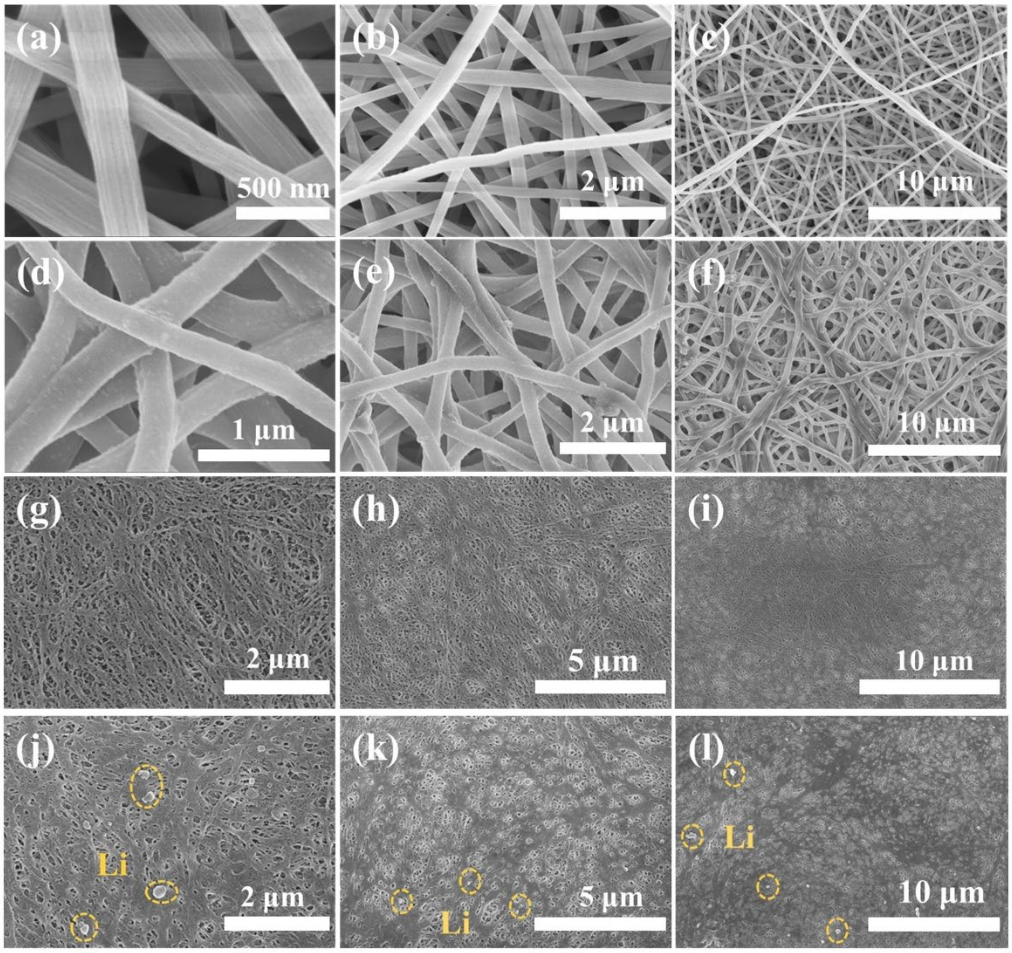

Figure S10. The top-view SEM images of pristine $LiFePO_4$ electrodes (a-d); and the top-view SEM images of the $LiFePO_4$ electrodes obtained in $LiFePO_4$/Li half cells assembled with PAN/CA composite nanofiber separators (e-h) and PE separators (i-l) after cycle performance test.

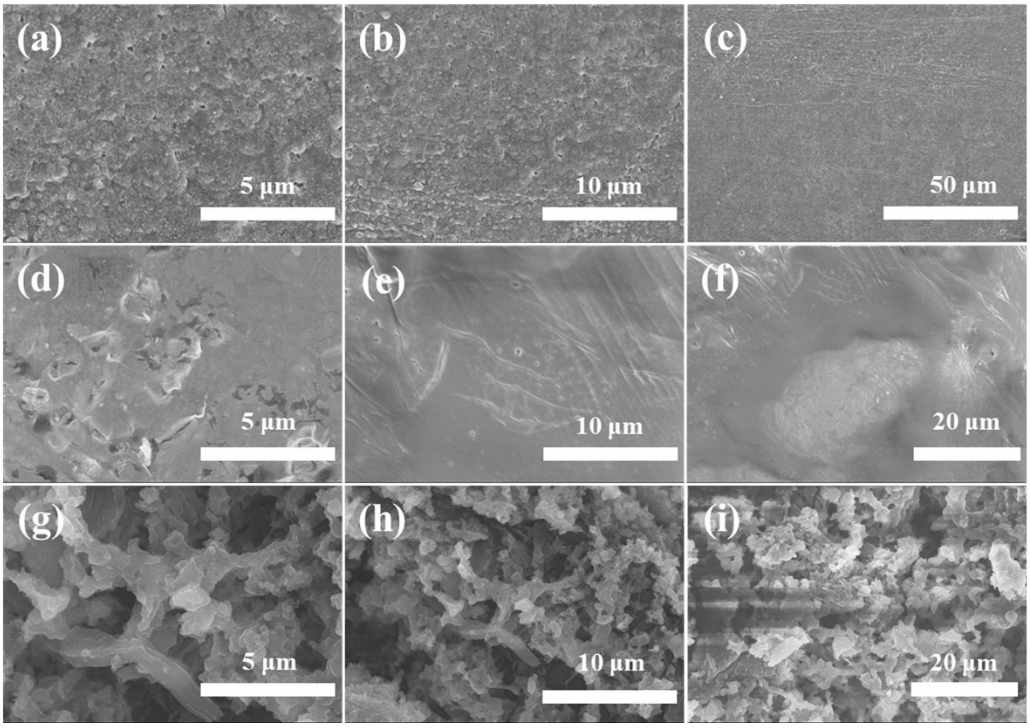

Figure S11. The top-view SEM images of (a-c) pristine PAN/CA composite nanofiber separators, (g-i) pristine PE separators. And the SEM images of (d-f) PAN/CA composited nanofiber separators and (j-l) PE separators disassembled from Li/Li symmetric cells after long-term cycles of Li plating/stripping process.

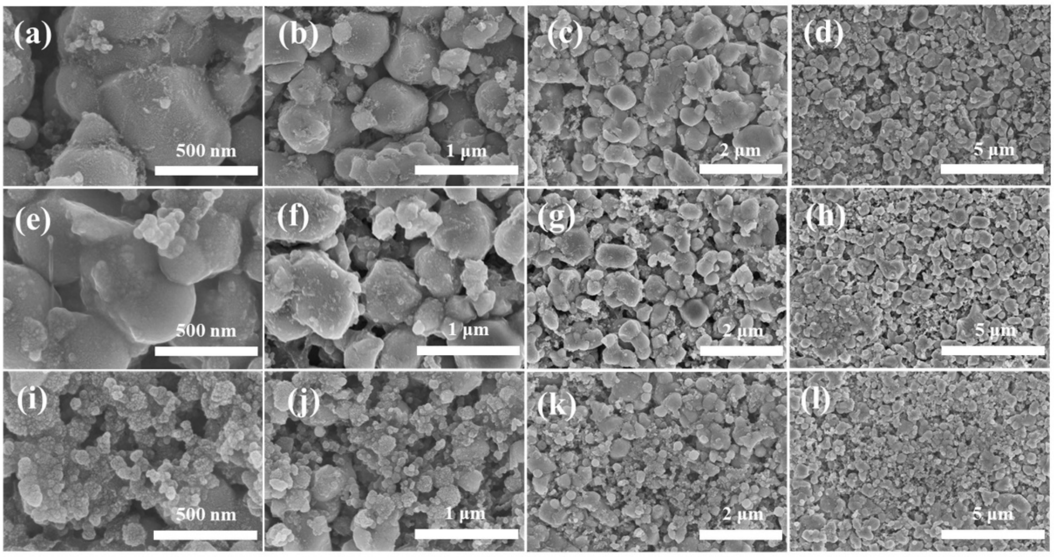

Figure S12. The top-view SEM images of fresh Li metal anodes (a-c), and the Li metal anodes obtained in $LiFePO_4$/Li half cells assembled with PAN/CA nanofiber separators (d-f) and PE separators (g-i) after cycle performance test.

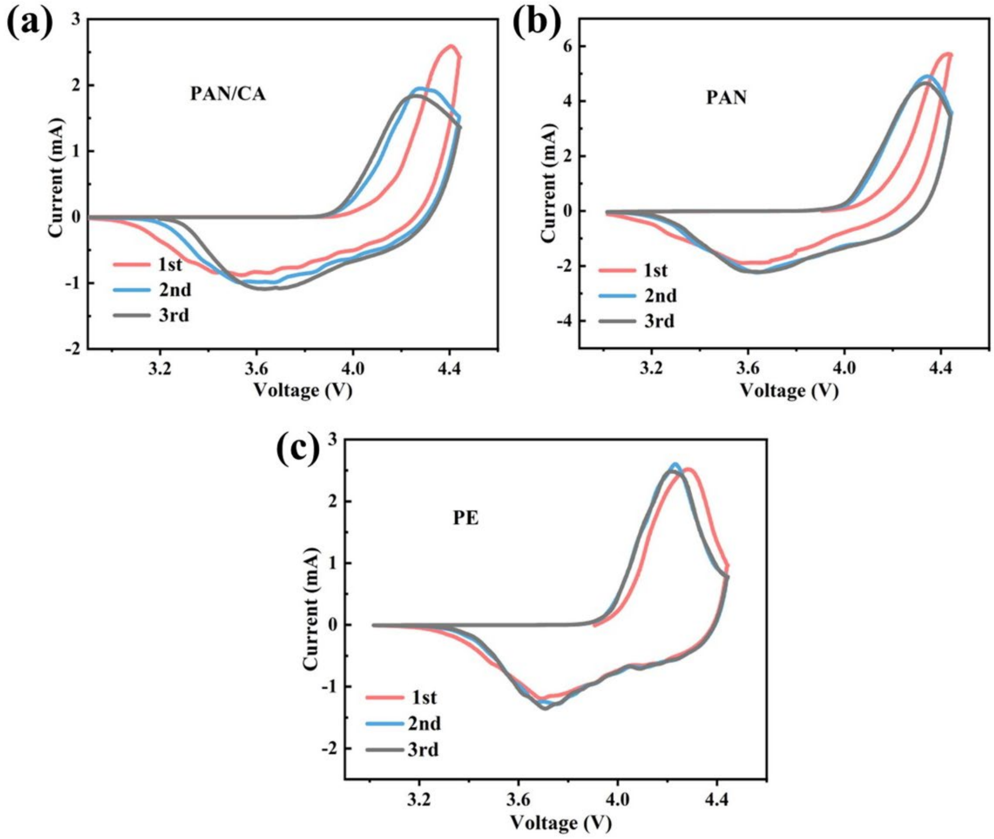

Figure S13. CV curves of $LiCoO_2$/Li battery based on (a) PAN/CA composite nanofiber separator, (b) PAN nanofiber separator and (c) PE separator.

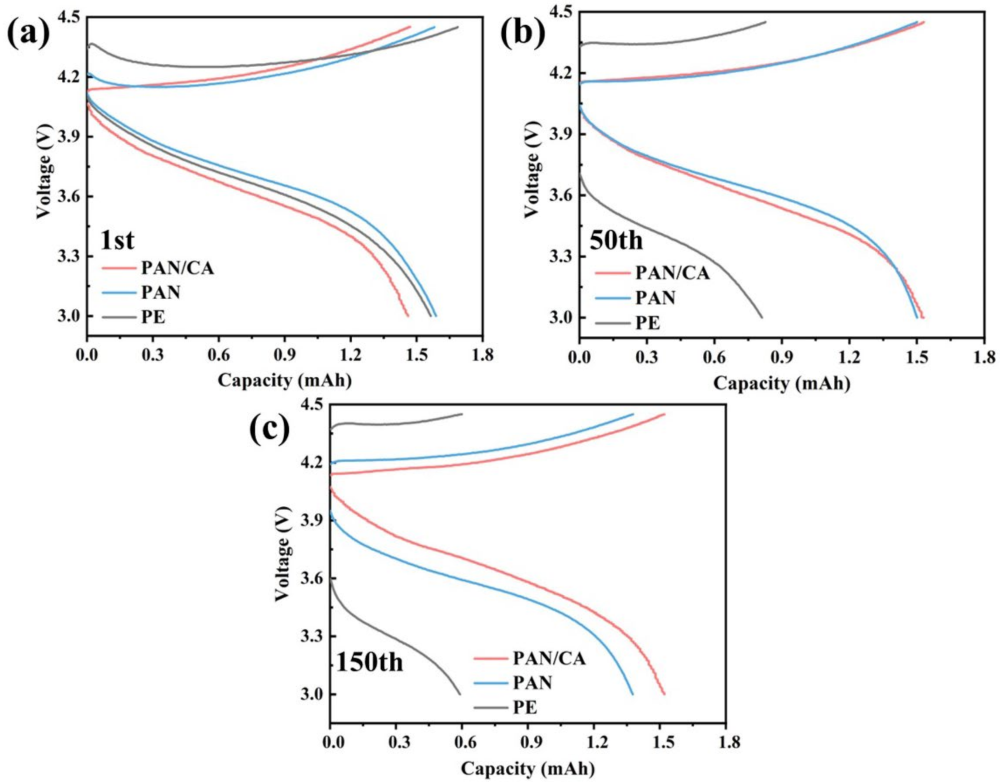

Figure S14. Discharge capacity -Voltage curves with different separators under different cycles: (a) 1st cycle; (b) 50th cycle; (c) 150th cycle.

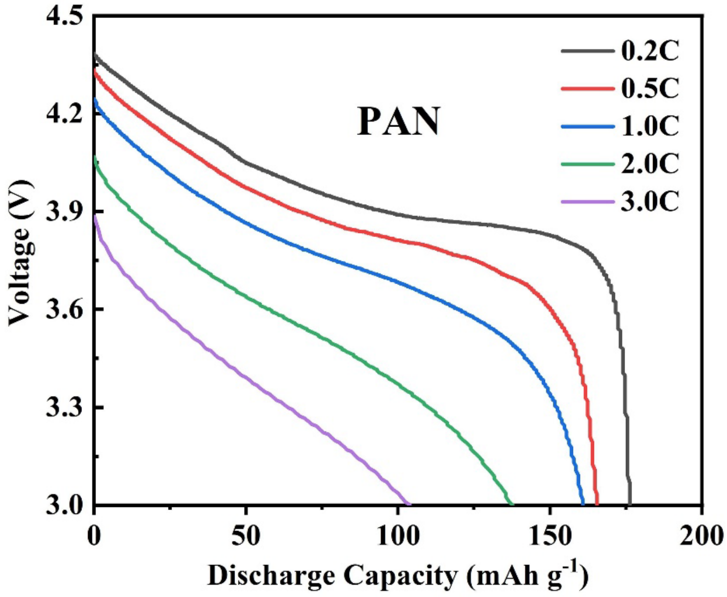

Figure S15. Discharge capacity-voltage curves of $LiCoO_2$/Li cells assembled with PAN nanofiber separator.

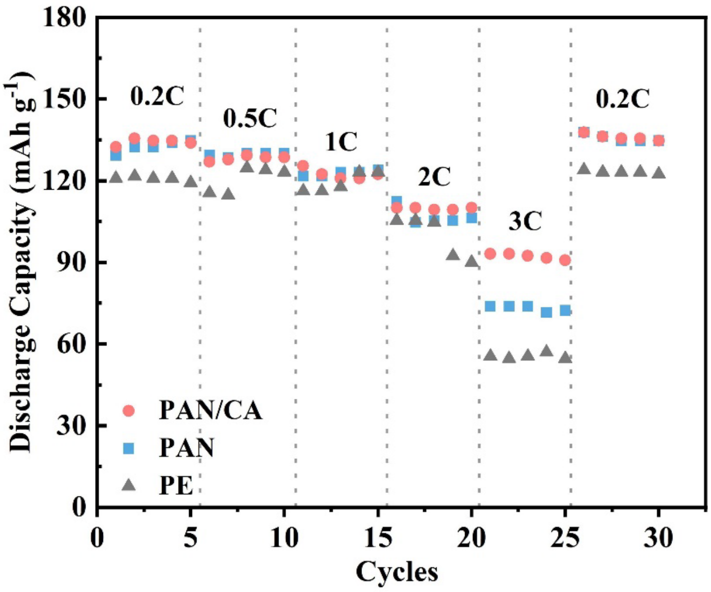

Figure S16. Rate performance of $LiFePO_4$/Li cells assembled with PAN/CA composite nanofiber separator, PAN nanofiber separator and PE separator.

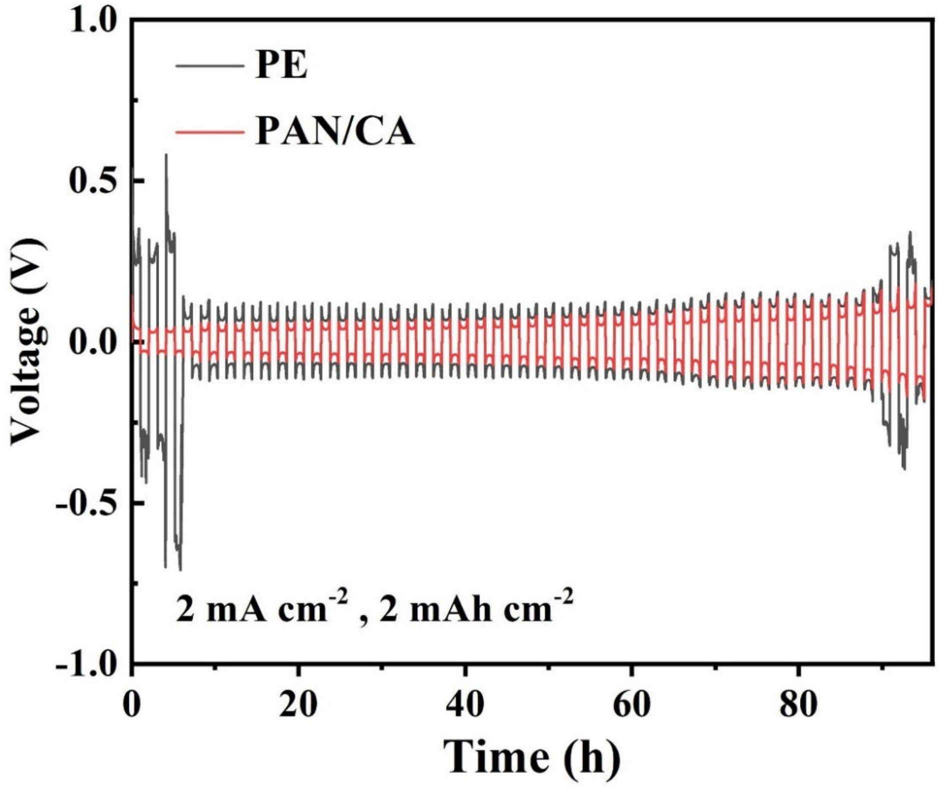

Figure S17. Charge-discharge voltage-time profiles of Li-symmetrical cells assembled with PAN/CA nanofiber separator and PE separator at current density of 2 mA cm^{-2} with an areal capacity of 2 mAh cm^{-2}.

Table S1. Performance comparison between the separators in this work and those reported in the Literature.

separator	condition	σ (ms cm^{-1})	capacity	ref.
PVDF-HFP/LAGP nanofiber separator	$LiNi_{0.8}Co_{0.1}Mn_{0.1}O_2$ with 6.0 mg cm^{-2}	from 0.70 to 3.18	144.7 mAh g^{-1}(84.5%) after 500 cycles; 0.2C	1
CCN separator	$LiFePO_4$	from 0.31 to 0.45	99.4 mAh g^{-1}(64.1%) after 300 cycles; 1C	2
PI/SiO_2 nanofiber separator	$LiNi_{0.8}Co_{0.1}Mn_{0.1}O_2$	from 0.52 to 1.55	149.6 mAh g^{-1} (88%) after 100 cycles; 1C	3
PAN nanofiber separator	$LiMn_2O_4$ with 16.6 mg cm^{-2}	from 0.59 to 1.06	89.5 mAh g^{-1} (99.4%) after 100 cycles; 0.5C	4
SiO_2/PAN cross-linked separator	$LiNi_{0.6}Co_{0.2}Mn_{0.2}O_2$ with 2.0 mAh cm^{-2}	from 0.46 to 2.10	162.1 mAh g^{-1} (94.0%) after 200 cycles; 0.5C	5
PI-COOH separator	$LiCoO_2$ with 11.9 mg cm^{-2}	from 2.11 to 2.50	103.7 mAh g^{-1} (98.8%) after 100 cycles; 0.5C	6
Co-SIM-1/PAN separator	$LiNi_{0.8}Co_{0.1}Mn_{0.1}O_2$	from 0.90 to 1.62	135.2 mAh g-1 (81.3%) after 250 cycles; 5C	7
PAN/CA nanofiber separator	**$LiCoO_2$ with 11.5 mg cm^{-2}**	**from 0.306 to 1.15**	**131.3 mAh g^{-1} (97.5%) after 300 cycles; 1C**	**This work**

Table S2. Physical properties of PAN/CA nanofiber separator, PAN nanofiber separator and PE separator.

Separator	PAN/CA	PAN	PE
Porosity (%)	61.47	82.54	33.51
Thickness (μm)	24	48	16
Tensile strength (Mpa)	11.36	3.26	86.35
Electrolyte uptake (%)	604.3	707.7	121.4

Reference

1 T. Liang, W. Liang, J. Cao, D. Wu, Enhanced Performance of High Energy Density Lithium Metal Battery with PVDF-HFP/LAGP Composite Separator, *ACS Applied Energy Materials*, 2021, **4**, 2578-2585.

2 T.W. Zhang, J.L. Chen, T. Tian, B. Shen, Y.D. Peng, Y.H. Song, B. Jiang, L.L. Lu, H.B. Yao, S.H. Yu, Sustainable Separators for High-Performance Lithium Ion Batteries Enabled by Chemical Modifications, *Adv. Funct. Mater*, 2019, **29**, 1902023.

3 D. Wu, N. Dong, R. Wang, S. Qi, B. Liu, D. Wu, In situ construction of High-safety and Non-flammable polyimide "Ceramic" Lithium-ion battery separator via SiO_2 Nano-Encapsulation, *Chem. Eng. J*, 2021, **420**, 129992.

4 X. Ma, P. Kolla, R. Yang, Z. Wang, Y. Zhao, A.L. Smirnova, H. Fong, Electrospun polyacrylonitrile nanofibrous membranes with varied fiber diameters and different membrane porosities as lithium-ion battery separators, *Electrochim. Acta*, 2017, **236**, 417-423.

5 S. Park, Y. Jung, W. Shin, K.H. Ahn, C.H. Lee, D. Kim, Cross-linked fibrous composite separator for high performance lithium-ion batteries with enhanced safety, *J. Membrane Sci*, 2017, **527**, 129-136.

6 C. Lin, H. Zhang, Y. Song, Y. Zhang, J. Yuan, B. Zhu, Carboxylated polyimide separator with excellent lithium ion transport properties for a high-power density lithium-ion battery, *J. Mater Chem A*, 2018, **6**, 991-998.

7 L. Yang, J. Cao, B. Cai, T. Liang, D. Wu, Electrospun MOF/PAN composite separator with superior electrochemical performances for high energy density lithium batteries,

Electrochim. Acta, 2021, **382**, 138346.